

Rationale for Using Irreversible Epidermal Growth Factor Receptor Inhibitors in Combination with Phosphatidylinositol 3-Kinase Inhibitors for Advanced Head and Neck Squamous Cell Carcinoma[□]

Nicole L. Michmerhuizen, Elizabeth Leonard, Chloe Matovina, Micah Harris, Gabrielle Herbst, Aditi Kulkarni, Jingyi Zhai, Hui Jiang, Thomas E. Carey, and J. Chad Brenner

Departments of Pharmacology (N.L.M., T.E.C., J.C.B.) and Otolaryngology—Head and Neck Surgery (N.L.M., E.L., C.M., M.H., G.H., A.K., T.E.C., J.C.B.), and Rogel Cancer Center (T.E.C., J.C.B.), University of Michigan Medical School, and Department of Biostatistics, University of Michigan School of Public Health (J.Z., H.J.), Ann Arbor, Michigan

Received November 5, 2018; accepted February 21, 2019

ABSTRACT

Head and neck squamous cell carcinoma (HNSCC) is a common and debilitating form of cancer characterized by poor patient outcomes and low survival rates. In HNSCC, genetic aberrations in phosphatidylinositol 3-kinase (PI3K) and epidermal growth factor receptor (EGFR) pathway genes are common, and small molecules targeting these pathways have shown modest effects as monotherapies in patients. Whereas emerging preclinical data support the combined use of PI3K and EGFR inhibitors in HNSCC, in-human studies have displayed limited clinical success so far. Here, we examined the responses of a large panel of patient-derived HNSCC cell lines to various combinations of PI3K and EGFR inhibitors, including EGFR agents with varying specificity and mechanistic characteristics. We confirmed the efficacy of PI3K and EGFR combination therapies, observing synergy with α isoform-selective PI3K inhibitor HS-173

and irreversible EGFR/ERBB2 dual inhibitor afatinib in most models tested. Surprisingly, however, our results demonstrated only modest improvement in response to HS-173 with reversible EGFR inhibitor gefitinib. This difference in efficacy was not explained by differences in ERBB target selectivity between afatinib and gefitinib; despite effectively disrupting ERBB2 phosphorylation, the addition of ERBB2 inhibitor CP-724714 failed to enhance the effect of HS-173 gefitinib dual therapy. Accordingly, although irreversible ERBB inhibitors showed strong synergistic activity with HS-173 in our models, none of the reversible ERBB inhibitors were synergistic in our study. Therefore, our results suggest that the ERBB inhibitor mechanism of action may be critical for enhanced synergy with PI3K inhibitors in HNSCC patients and motivate further preclinical studies for ERBB and PI3K combination therapies.

Introduction

Head and neck squamous cell carcinoma (HNSCC) represents the sixth most common form of cancer by incidence worldwide and is often associated with either high alcohol and tobacco use or infection with high-risk human papilloma virus (HPV) (Kamangar et al., 2006) (https://seer.cancer.gov/archive/csr/1975_2013/). The disease has 5-year survival rates of less than 50% for HPV-negative tumors and around 80% for HPV-positive tumors, and we believe that overall survival for patients will be improved by advancing novel therapeutic approaches that target aberrations common to

different subsets of HNSCC tumors (Giefing et al., 2016; Ludwig et al., 2016). Furthermore, the development of effective, rational combination therapies may be critical for overcoming common resistance mechanisms that emerge after targeted monotherapy. We believe this approach may have utility for both adapting clinical paradigms with adjuvant/neoadjuvant agents, as well as advancing personalized medicine approaches through the development of rational combination therapies for the most prominent molecular alterations in HNSCC.

Of the potential targetable molecular alterations common to HNSCC, the phosphoinositide-3 kinase (PI3K) pathway is disrupted through genomic amplifications or activating point mutations in >30% of tumors (Lui et al., 2013; Murugan et al., 2013; Gillison et al., 2015; Michmerhuizen et al., 2016), and the epidermal growth factor receptor (EGFR) is overexpressed in >90% of tumors (Ozanne et al., 1986; Lui et al., 2013; Gillison et al., 2015). Inhibitors to each of these pathways have already been advanced individually in HNSCC. For example,

This work was supported by the National Institutes of Health National Institute of Dental and Craniofacial Research (Grant U01-DE025184) and National Cancer Institute (Grant R01-CA194536), the National Science Foundation (Grant DGE-1256260), and funds from the American Head and Neck Society.

<https://doi.org/10.1124/mol.118.115162>.

[□] This article has supplemental material available at molpharm.aspetjournals.org.

ABBREVIATIONS: AKT, protein kinase B; ANOVA, analysis of variance; DMSO, dimethylsulfoxide; EGFR, epidermal growth factor receptor; ERK, extracellular signal-regulated kinase; FITC, fluorescein isothiocyanate; HNSCC, head and neck squamous cell carcinoma; HPV, human papilloma virus; MEK, methyl ethyl ketone; PBS, phosphate-buffered saline; PI3K, phosphatidylinositol 3-kinase.

in a recent phase 2 trial, pan-PI3K inhibitor BKM120 (buparlisib) with paclitaxel improved survival compared with paclitaxel and placebo in recurrent and metastatic HNSCC patients (Soulières et al., 2017), and EGFR antibody cetuximab is currently in clinical use after demonstrating improved outcomes in combination with radiotherapy or cisplatin (Bonner et al., 2006; Vermorken et al., 2008). Thus, although PI3K and EGFR targeting therapies have been used with some clinical success, response rates are still relatively low, and innate or acquired resistance mechanisms appear to be widespread (Bonner et al., 2006; Vermorken et al., 2008; Boeckx et al., 2013; Rodon et al., 2014; Michmerhuizen et al., 2016; Soulières et al., 2017).

Preclinical data indicate that dual therapies directed against both PI3K and EGFR pathways might improve responses in HNSCC (Rebucci et al., 2011; Young et al., 2013; D'Amato et al., 2014; Lattanzio et al., 2015; Michmerhuizen et al., 2016; Anisuzzaman et al., 2017; Silva-Oliveira et al., 2017). Given these promising data, several clinical trials assessing the combination in HNSCC have been opened, most of which use the EGFR-targeting antibody cetuximab in combination with various inhibitors of PI3K (e.g., NCT01816984, NCT2282371, NCT02822482). Unfortunately, however, one study showed no significant improvement in patient survival with the addition of pan-PI3K inhibitor PX-866 to cetuximab (Jimeno et al., 2015). These surprising data suggested that a deeper understanding of the molecular mechanisms of action that drive response to PI3K and EGFR therapies is necessary to fully interpret the results of these trials.

Here, because of the early reported disparity between in vitro and clinical trial results, we conducted further studies characterizing the responses to various classes of PI3K and EGFR dual therapies in HNSCC. We used a panel of genetically diverse HNSCC cell lines to examine responses to combinations of PI3K and EGFR inhibitors; in doing so, we sought to assess patterns of response that might translate to future clinical trial design and/or serve as a guide for future precision medicine protocols in HNSCC.

Materials and Methods

Cell Culture. Cells were cultured in a humidified incubator at 37°C with 5% (vol/vol) CO₂. UM-SCC cells (University of Michigan) and human tumor cell line Cal-33 cells (a kind gift from Dr. Anthony Nichols) were previously derived from HNSCC patient tumor samples and cultured in Dulbecco's modified Eagle's medium with 10% fetal bovine serum, 1× penicillin/streptomycin, 1× nonessential amino acid (Brenner et al., 2010). HSC-2, HSC-4 (both from Japanese Collection of Research Bioresources through Sekisui XenoTech, Kansas City, KS), and Detroit 562 (American Type Culture Collection, Manassas, VA) cells were cultured in Eagle's minimum essential medium with 10% fetal bovine serum, 1× penicillin/streptomycin. All cell lines were genotyped to confirm authenticity and were mycoplasma-negative.

Details of DNA copy number analysis are published elsewhere (Ludwig et al., 2018). All UM-SCC cell lines were confirmed to contain *PIK3CA*, as previously reported from Nimblegen V2 exome capture-based experiments (Liu et al., 2013). Cal-33, HSC-2, and HSC-4 copy number data were obtained from the publicly available canSAR database (Halling-Brown et al., 2012; Bulusu et al., 2014). *EGFR* mutation status or copy number was similarly assessed using data from Nimblegen V2 exome capture-based experiments (Liu et al., 2013) for UM-SCC cell lines; the canSAR database for HSC-2, HSC-4, and Cal-33 (Halling-Brown et al., 2012; Bulusu et al., 2014); and previously published work for Detroit 562 (Young et al., 2013).

Genomic DNA Purification. Cells from models with *PIK3CA* mutations (Cal-33, HSC-2, HSC-4, Detroit 562, UM-SCC-43, UM-SCC-19, UM-SCC-85) were harvested and washed in phosphate-buffered saline (PBS) and then frozen at -20°C. The thawed cell pellet was resuspended in 700 μ l of Nuclei Lysis solution (Promega, Madison, WI) for 1 hour at 55°C. Then 200 μ l of Protein Precipitation solution (Promega) was added to the sample, which was mixed and placed on ice for at least 5 minutes before being centrifuged at 13,000 rpm and 4°C for 5 minutes. The supernatant was transferred to a tube containing 600 μ l of isopropanol and centrifuged at 13,000 rpm for 1 minute. After aspirating the resulting supernatant, the DNA pellet was washed in 200 μ l of 70% ethanol, dried, and resuspended in 30–50 μ l of nuclease-free water.

Sanger Sequencing. Genomic DNA was amplified using polymerase chain reaction (PCR) with Platinum *Taq* DNA Polymerase High Fidelity (Invitrogen, Carlsbad, CA) according to the manufacturer's instructions and the primers with sequences listed in Supplemental Fig. 1. After being inserted into the pCR8 vector system or processed using the Qiagen QIAquick PCR purification kit, PCR products were submitted for Sanger sequencing at the University of Michigan DNA Sequencing Core on the 3730XL DNA Sequencer (Applied Biosystems, Foster City, CA) as described elsewhere (Birkeland et al., 2017). Sequences were aligned using the DNASTAR Lasergene software suite (DNASTAR, Inc, Madison, WI).

Chemicals. All compounds (BYL719, HS-173, BKM120, afatinib, gefitinib, erlotinib, BMS-599626, AEE788, TAK-285, CUDC-101, and dacomitinib) were purchased from Selleck Chemicals (Houston, TX). Each inhibitor was initially dissolved in 100% sterile dimethylsulfoxide (DMSO) to 10 mM and then diluted in media to the indicated concentrations for studies in vitro. Table S2 gives the chemical name for each inhibitor used here.

Resazurin Cell Viability Assay. Resazurin cell viability assays were performed as described previously (Shum et al., 2008; Birkeland et al., 2016; Michmerhuizen et al., 2016). To study relative cell viability, 2000 cells/well (for all cell lines except HSC-2, for which the cell density was reduced to 1000 cells/well owing to large cell size and rapid growth rate) were seeded (in 50 μ l volume) in 384-well microplates using a Biotek (Winooski, VT) Multiflo liquid-handling dispensing system. Cells adhere overnight before treatment. Inhibitors were prepared by hand from 10 mM stocks at 200× concentration in a 96-well plate, then diluted 10× concentration in media in a second 96-well plate using the Agilent (Santa Clara, CA) Bravo Automated Liquid Handling Platform and VWorks Automation Control Software. The intermediate plate with inhibitors in media was used to treat the cells with the desired compound concentration, again using liquid-handling robotics such that cells were treated with complete media containing 0.5% inhibitor or DMSO in a 10-point 2-fold dilution series. Each treatment was administered in quadruplicate. Cells were stained with 10 μ l of 440 μ M resazurin (Sigma, St. Louis, MO) dissolved in serum-free media for 12–24 hours before fluorescent signal intensity was quantified. Quantification occurred after 72-hour treatment using the Biotek Cytation3 fluorescence plate reader at excitation and emission wavelengths of 540 and 612 nm, respectively. Data were plotted using Prism 7 and fit with concentration response curves using the log(inhibitor) versus response-variable slope model with four parameters (IC₅₀, top, bottom, and Hill slope) allowed to vary.

Annexin V Apoptosis Assay. To study annexin V presentation, 115,000 Detroit 562 cells or 100,000 UM-SCC-59 cells/well were seeded in six-well plates. After 24 hours, media were aspirated and replaced with 3 ml of fresh, complete media. One milliliter of media containing DMSO or inhibitor(s) was added to each well. Cells were cultured for 72 hours, at which time, media were collected from each well. Each well was then washed in PBS, which was also collected. Finally, cells were trypsinized and added to the suspension. Samples were then centrifuged, washed once with PBS, and counted using the Countess Automated Cell Counter (Invitrogen). One hundred thousand cells/sample were stained with annexin V fluorescein isothiocyanate (FITC) and phosphatidylinositol using the Dead Cell Apoptosis Kit (ThermoFisher, Waltman, MA)

according to manufacturer's instructions. Five microliters of annexin V FITC and 5 μ l of phosphatidylinositol were added to each sample. Samples were incubated at room temperature in the dark for 15 minutes and analyzed using the Bio-Rad ZE5 or MoFlo Astrios EQ Cell Sorter at the University of Michigan Flow Cytometry Core.

Western Blotting. Cells at 70%–80% confluency were treated with DMSO or inhibitor before harvesting and lysing in radioimmunoprecipitation assay buffer (cat. no. 89900; ThermoFisher) containing 1% NP-40 and 0.1% SDS. Eight to 20 μ g of each cell harvest was used, and standard Western blot protocols were followed as previously described (Birkeland et al., 2016). Primary antibodies (described in detail in Supplemental Table 1) were incubated overnight at 4°C or for at least 1 hour at room temperature, followed by a goat anti-rabbit horseradish peroxidase (cat. no. 111-035-045; Jackson ImmunoResearch, West Grove, PA) secondary antibody at room temperature for 1 hour as described elsewhere (Tillman et al., 2016). The blots were then visualized with chemiluminescence and imaged. Three hundred dots per inch or greater images were digitally retained from all Western blots, and representative blots are shown. ImageJ software (NIH) was used to quantify protein expression and compare treatment responses.

Synergy Analysis. The effects of combination treatments were analyzed with Combeneft software (Di Veroli et al., 2016) using the highest single agent model (Bliss, 1939; Berenbaum, 1981; Greco et al., 1995; Borisy et al., 2003; Mathews Griner et al., 2014). For each cell line and pair of inhibitors, the number of concentration combinations with scores >20 was counted. These counts were averaged across at least two (and as many as five) independent replicates for each experiment. Experiments having more than eight concentration combinations with scores >20 were considered additive or synergistic. We compared the number of concentration combinations with scores >20 for HS-173 and afatinib (afatinib combination score), as well as HS-173 and gefitinib (gefitinib combination score). Cell lines were considered more responsive to the afatinib combination if the afatinib combination score exceeded the gefitinib combination score by eight or more.

Statistical Analysis. To determine whether statistically significant differences occurred with combination treatments, a two-way analysis of variance (ANOVA) was performed in R to compare the natural logarithm of the percentage of living cells after vehicle, HS-173, gefitinib or afatinib, or combination treatment. Specifically, this test was performed using type III analysis with the ANOVA function from the “car” package. The interaction between HS-173 and gefitinib or afatinib treatment indication was tested by F-test for the synergy effect of drug combination. In total, four separate tests on drug combination (HS-173 combined with gefitinib or afatinib for UM-SCC-59 and Detroit 562 cell lines) were performed simultaneously; so Bonferroni correction was used to adjust *P* values.

Results

Subsets of HNSCCs Respond to PI3K + EGFR Inhibitor Combination Therapies. To first probe the dependence of HNSCC cell lines to PI3K and EGFR pathway inhibitors, we compared the response of a small panel of models to the PI3K α inhibitor HS-173 (Lee et al., 2013; Rumman et al., 2016) and irreversible pan-EGFR/ERBB2 inhibitor afatinib (Li et al., 2008) as monotherapies and in combination. We selected HS-173 as the PI3K inhibitor as it was the most effective and isoform-selective small molecule in our panel of cell lines. Afatinib was used as the ERBB inhibitor; this drug was approved by the Food and Drug Administration in 2016 as a first-line treatment of patients with non-small-cell lung cancer whose tumors harbored mutations in EGFR. It has also displayed efficacy in HNSCC (NCT00514943) and is being evaluated in ongoing studies using various paradigms (NCT01824823,

NCT01415674, NCT01427478, NCT02979977). PI3K and ERBB inhibitor combination experiments were performed in four models with *PIK3CA* mutations (HSC-2, HSC-4, Detroit 562, and Cal-33; Supplemental Fig. 1) and one with high-level *PIK3CA* amplification (UM-SCC-59, five wild-type copies) using a resazurin cell viability assay after 72-hour drug treatment and then validated by annexin V apoptosis assay (below). Our studies showed variable responses by cell line.

HSC-2, HSC-4, and Detroit 562 display a hotspot *PIK3CA* mutation (indicating activation of and likely dependence on the PI3K signaling pathway) but have limited responses to HS-173 and other PI3K inhibitors as monotherapies, with IC₅₀ close to or exceeding 1 μ M. In these three cell lines, we observed that the addition of afatinib to HS-173 resulted in dose-dependent improvements in the efficacy of PI3K inhibition (Fig. 1, A–C). These results represented drug synergy using the highest single agent model. This effect was also observed when pan-PI3K inhibitor BKM120 and another PI3K α inhibitor, BYL719, were titrated with afatinib (Supplemental Fig. 2, A and B) but not when p110 β inhibitor TGX-221 was tested in combination (Supplemental Fig. 2C), suggesting that the synergistic dose-combination response specifically requires inhibition of PI3K α . Similarly, titrating afatinib into constant concentrations of HS-173 or BKM120 resulted in synergistic responses in combination-responsive *PIK3CA* mutant cell lines HSC-4 and Detroit 562 (Supplemental Fig. 3). In contrast, the data also demonstrated that one of the *PIK3CA* mutant HNSCC cell lines, Cal-33, as well as the *PIK3CA*-amplified cell line, UM-SCC-59, showed little combination benefit (Fig. 1, D and E), suggesting that these models depend on alternative survival pathways.

After establishing that subsets of HNSCCs responded synergistically to HS-173 and afatinib, we examined the downstream signals in the PI3K and EGFR pathways to identify potential differences in signaling transduction pathways between two combination-responsive models (HSC-2 and Detroit 562) and one combination nonresponsive model (Cal-33). Thus, after a 6-hour treatment with vehicle (DMSO), HS-173 monotherapy, afatinib monotherapy, or HS-173 and afatinib combination therapy, we evaluated EGFR and ERBB2 phosphorylation, as well as effector signaling through protein kinase B (AKT), MAPK/ERK kinase (mitogen-activated protein kinase/extracellular signal-regulated kinase kinase, MEK), and extracellular signal-regulated kinase (ERK) (Fig. 2). As expected, afatinib monotherapy could inhibit EGFR and ERBB2 phosphorylation. Although the degree of reduction that afatinib reduced ERBB2 phosphorylation in lysates from treated Detroit 562 cells was fairly minimal, more robust effects on ERBB2 phosphorylation are visible after shorter treatment times (likely due to transient effects on receptor phosphorylation; see Fig. 3C below). Downstream of these effects on EGFR and ERBB2 signaling, ERK and MEK phosphorylation are similarly decreased in nonresponsive Cal-33 and responsive HSC-2 cell lines. Detroit 562 cells display minimal changes in MEK phosphorylation after treatment at this dose and time point, yet ERK phosphorylation is reduced somewhat. AKT phosphorylation, used as a readout of primarily PI3K but also EGFR pathway activity, was reduced in HS-173 monotherapy-treated samples in each cell line. In the responsive HSC-2 cell line, a further reduction in AKT phosphorylation was evidenced

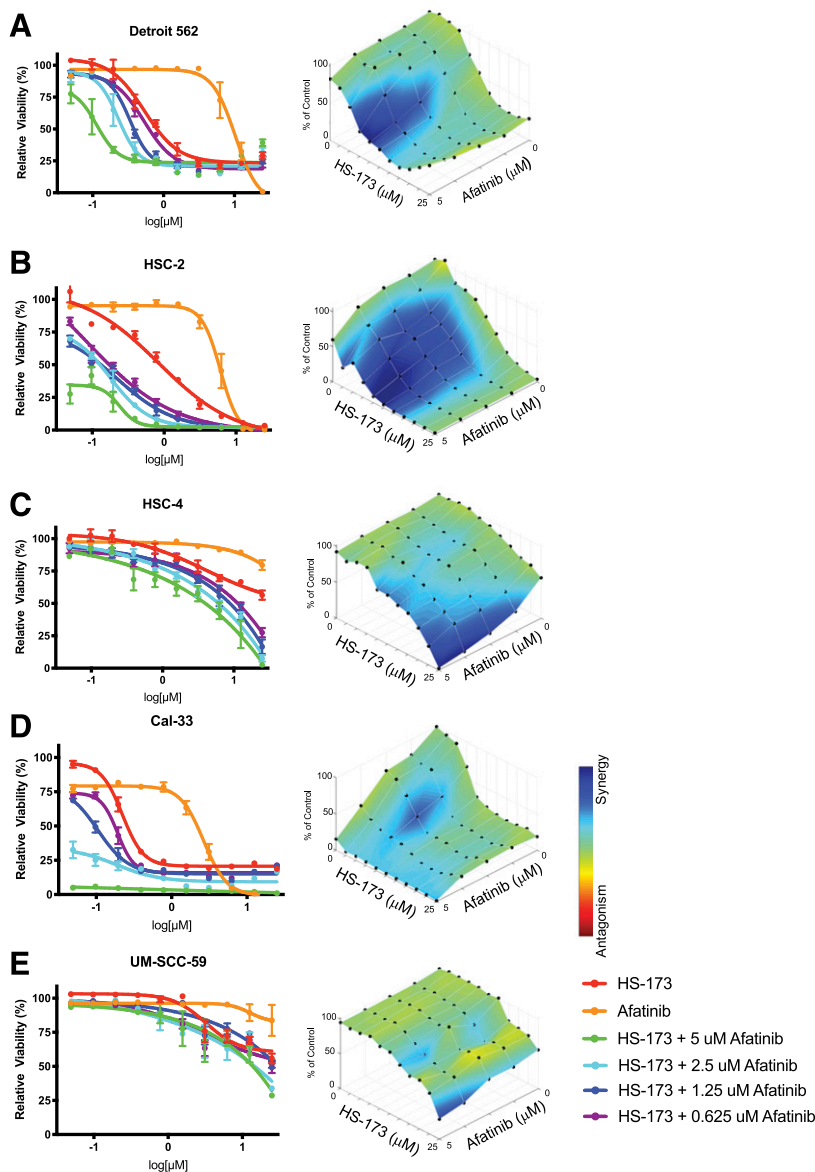


Fig. 1. Responses to HS-173 + afatinib treatment in HNSCC cell lines. (A) Detroit 562, (B) HSC-2, (C) HSC-4, (D) Cal-33, and (E) UM-SCC-59 were treated with increasing concentrations of PI3K α inhibitor HS-173 and/or EGFR/ERBB2 inhibitor afatinib for 72 hours. Cell viability was measured using a resazurin cell viability assay. Each point is the mean and S.D. of quadruplicate determinations from a single experiment. Each experiment was repeated independently at least three times with similar combination effects; representative data are shown along with analysis using Combenefit software (Di Veroli et al., 2016).

with the addition of afatinib to HS-173. Thus, in non-responsive and responsive models, inhibition of PI3K's downstream signaling through AKT and inhibition of ERBB signaling both at the receptor level and downstream through MEK and ERK was achieved (Fig. 2), indicating that the combination effect was not limited to models with reductions in effector signaling.

Responses to PI3K + EGFR Inhibition Vary Based on Inhibitor Type. We further investigated the role of ERBB inhibition in HS-173 and afatinib combination response by testing PI3K α inhibitor HS-173 in combination with reversible EGFR inhibitor gefitinib in the responsive PI3K mutant HNSCC models Detroit 562 and HSC-2. Resazurin cell viability experiments performed displayed a much less marked effect with HS-173 and gefitinib compared with cotreatment with HS-173 and afatinib (Fig. 3, A and B). These effects were confirmed using an orthogonal annexin V apoptosis assay. For example, in the Detroit 562 cell line (synergistically responsive to HS-173 and afatinib), we observed higher levels of FITC-positive (apoptotic) cells after

di-therapy compared with what would be expected from additive effects of HS-173 and afatinib monotherapies (adjusted P value = 0.009, two-way ANOVA). Importantly, no significant change in cell death was seen in the non-synergistically responsive UM-SCC-59 model (adjusted P value = 1, two-way ANOVA), and HS-173 combinations with gefitinib were ineffective in both cell lines (adjusted P values = 1, two-way ANOVA) (Fig. 4). These data suggested a significant difference in the ability of gefitinib and afatinib to induce synergistic cell kill in our models.

Given this surprising observation, we expanded our original analyses on five cell lines with a larger panel of HNSCC models. Here, we selected an additional nine models with genetic characteristics of tumors most likely to receive PI3K or EGFR inhibitors in a precision medicine setting, including those with either *PIK3CA* mutations or high-level gene amplifications (>4 copies). Consistent with our previous data (Michmerhuizen et al., 2016), the additivity between HS-173 and gefitinib was observed in only 4 of 14 (29%) of models (Fig. 5A).

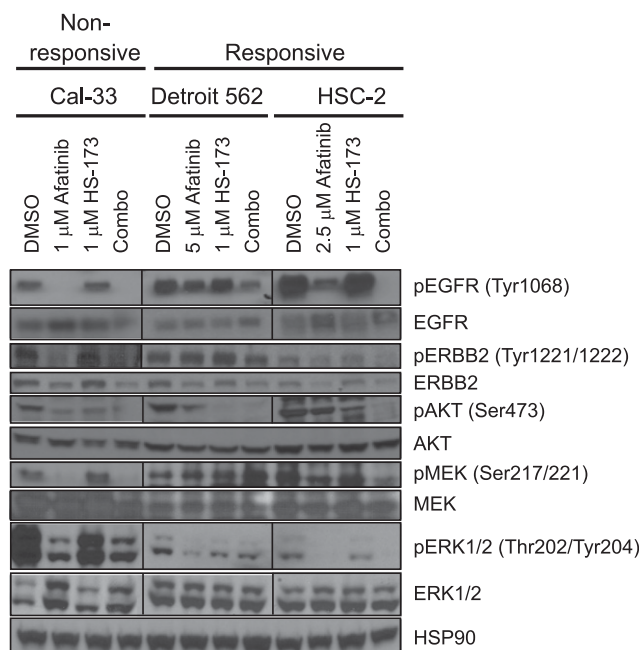


Fig. 2. Signaling responses to HS-173 + afatinib in combination responsive and nonresponsive HNSCC cell lines. Western blot analysis of downstream PI3K and RAS-MEK-ERK pathway activation after 6-hour treatment with vehicle (DMSO), EGFR/ERBB2 inhibitor afatinib, PI3K α inhibitor HS-173, and a combination in Cal-33, Detroit 562 and HSC-2 cell lines. HSP90 was used as a loading control. Representative images are shown.

Importantly, much more significant “further benefit,” which we define as including multiple synergistic dose combinations, was observed with HS-173 and afatinib combination therapy

in 8 of 14 (57%) of models (Fig. 5A). Of the four models that demonstrated additivity with gefitinib, three received further benefit with afatinib. The in vitro models that failed to display robust improvements in response to HS-173 with the addition of afatinib included Cal-33 (Fig. 1D), UM-SCC-59 (Fig. 1E), UM-SCC-19, UM-SCC-43, and UM-SCC-85 (Fig. 5A). Cal-33, UM-SCC-19, UM-SCC-43, and UM-SCC-85, like some of the combination-responsive models discussed herein, display activating mutations in *PIK3CA* (Supplemental Fig. 1). Cal-33 and UM-SCC-85 cells were among the most sensitive to PI3K inhibitor monotherapies, whereas UM-SCC-59 (with high-level amplification of wild-type *PIK3CA*) is one of the most resistant. Thus, neither *PIK3CA* mutation nor responsiveness to PI3K inhibitor monotherapy is a good predictor of responsiveness to HS-173 and afatinib cotreatment. Likewise, at least when considered as single variables, *PIK3CA* copy number (Fig. 5A), *EGFR* copy number (Fig. 5A), and ERBB2 protein expression (Fig. 5B) are also poor indicators of combination response. Although mutations in *EGFR* are closely linked to responses to EGFR inhibitors (Lynch et al., 2004; Paez et al., 2004; Yu et al., 2013, 2015; Thress et al., 2015; Wu et al., 2016), the cell lines used here did not display such variants. Thus, neither sensitivity nor resistance to EGFR inhibitor monotherapies or combination therapies can be explained by the presence of L858R or T790M/C797S mutations, respectively. After our resazurin assay determined that the HS-173 and gefitinib combination was largely ineffective compared with HS-173 and afatinib, we tested the combination of HS-173 and afatinib in UM-SCC-110 and patient-matched fibroblasts and demonstrated the inability of combination therapy to drive cell death in normal fibroblasts (Supplemental Fig. 4).

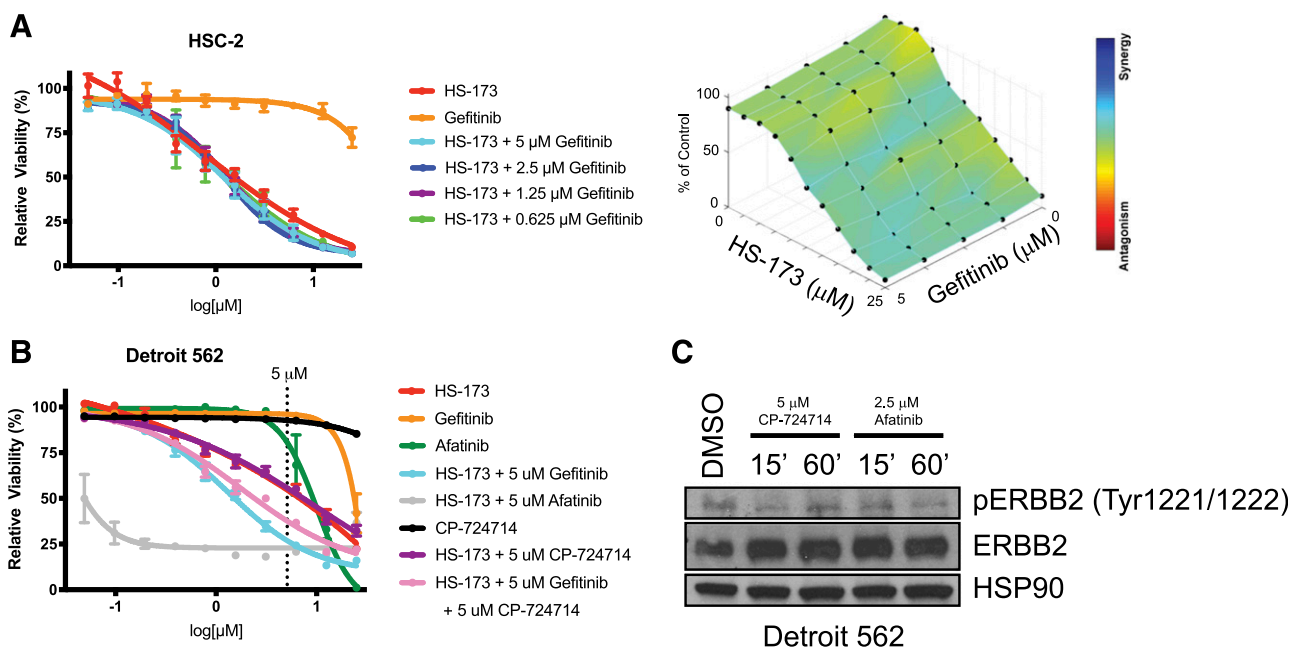


Fig. 3. Responses to HS-173 + ERBB inhibitor treatment in *PIK3CA* mutant HNSCC cells. (A) HSC-2 cells were treated with increasing concentrations of PI3K α inhibitor HS-173 and/or EGFR inhibitor gefitinib for 72 hours. Cell viability was measured using a resazurin cell viability assay. Each point is the mean and S.D. of quadruplicate determinations from a single experiment. Each experiment was repeated independently at least three times with similar combination effects; representative data are shown along with analysis using Combeneft software (Di Veroli et al., 2016). (B) Detroit 562 cells were treated with increasing concentrations of PI3K α inhibitor HS-173 and/or EGFR gefitinib, ERBB2 inhibitor CP-724714, and/or EGFR/ERBB2 inhibitor afatinib for 72 hours. Cell viability was measured using a resazurin cell viability assay. Each point is the mean and S.D. of quadruplicate determinations from a single experiment. This experiment was repeated independently three times with similar combination effects; representative data are shown. (C) Western blot analysis of phosphorylated and total ERBB2 expression after treatment with vehicle (DMSO) or 15- or 60-minute treatment with either ERBB2-specific inhibitor CP-724714 or EGFR/ERBB2 inhibitor afatinib in Detroit 562 cells. HSP90 was used as a loading control.

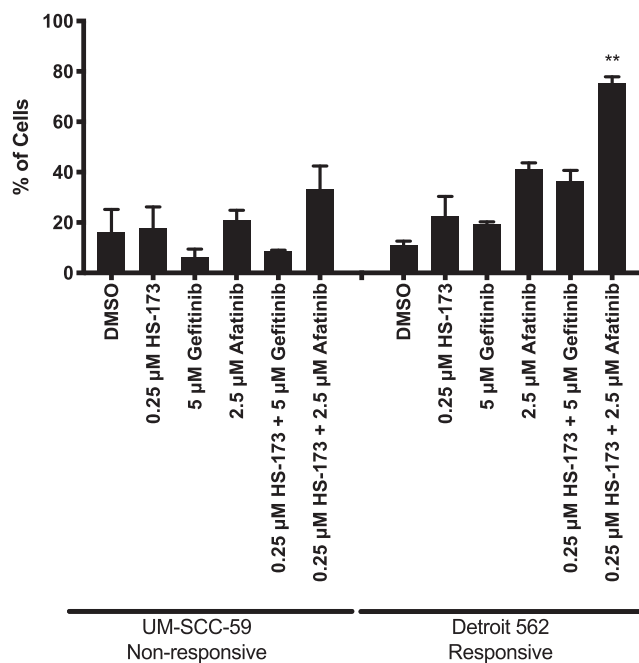


Fig. 4. Cell-death responses to HS-173 + afatinib treatment in combination responsive and nonresponsive HNSCC cell lines. Combination non-responsive model UM-SCC-59 and combination responsive model Detroit 562 were treated with vehicle (DMSO), PI3K α inhibitor HS-173, reversible EGFR inhibitor gefitinib, and/or EGFR/ERBB2 irreversible inhibitor afatinib for 72 hours. Cell viability was measured using an annexin V apoptosis assay after cells were stained with FITC and PI. Data shown represents the mean and S.D. from two to three independent experiments. **Significance with $P < 0.01$ using two-way ANOVA to compare vehicle, HS-173, afatinib, and combination, as described in *Materials and Methods*. Comparisons for HS-173 and gefitinib combinations in each cell line and for HS-173 and afatinib combination in UM-SCC-59 were performed but are not shown given the lack of significant interaction term.

Together, these data strongly suggest important differences between afatinib- and gefitinib-based combinations in our model system. Given the differences between the inhibitors, we hypothesized that the greater effectiveness with afatinib over gefitinib may be due to 1) a broader spectrum of ERBB family member inhibition and/or 2) irreversible as opposed to reversible inhibition of EGFR. To begin testing this hypothesis using combination responsive Detroit 562 cells, we performed a resazurin cell viability assay in which we compared the effects of HS-173 and gefitinib with or without ERBB2-specific inhibitor CP-724714 (Fig. 3B). This assay demonstrated that CP-724714 was unable to add to HS-173 and gefitinib in this assay, and the total effect of this tritherapy combination remained much less substantial than the effect of HS-173 and afatinib. This result suggested the possibility that ERBB2 inhibition did not account for the differences between inhibitors or that CP-724714 could not sufficiently inhibit ERBB2 signaling in our system.

Consequently, to validate that the doses of CP-724714 used here could sufficiently inhibit ERBB2 signaling, we performed Western blot analysis on lysates harvested from Detroit 562 cells after CP-724714 or afatinib treatment. At doses equivalent to or less than those used in resazurin cell viability assays, we observed that both CP-724714 and afatinib treatment resulted in robust inhibition of ERBB2 phosphorylation after 15 or 60 minutes (Fig. 3C). We also examined lysates from HSC-2 cells after 2-hour treatment with each monotherapy

or ditherapy (Fig. 5C). This demonstrated decreased EGFR phosphorylation in gefitinib- and afatinib-treated samples, with a slightly greater loss of EGFR phosphorylation with afatinib than gefitinib. Phosphorylation of ERK, GAB1, and MEK, downstream of EGFR, were similar for gefitinib and afatinib treatments; in addition, cotreatment with HS-173 and gefitinib or afatinib did not reduce downstream ERBB signals beyond those levels seen with gefitinib and afatinib monotherapy treatments. Phosphorylation of PI3K pathway effector AKT was appropriately inhibited upon HS-173 treatment, but PDK1 and GSK3 β phosphorylation remained unchanged. Together, these data suggest that ERBB2 inhibition alone may not explain the differences between the gefitinib and afatinib combinations and therefore warrant further evaluation of differences between reversible and irreversible ERBB inhibitor combinations.

Thus, using a resazurin cell-viability assay, we tested HS-173 in combination with three reversible ERBB inhibitors (erlotinib, BMS-599626, and CP-724714) and three irreversible ERBB-targeting agents (TAK285, CUDC-101, and dacomitinib) in HSC-2 and Detroit 562 cells. Although we observed that none of the four (0%) reversible ERBB inhibitors displayed synergistic dose combinations in either cell line, three of four (75%) and four of four (100%) irreversible ERBB-targeting drugs had synergistic dose combinations with HS-173 in Detroit 562 and HSC-2 cells, respectively (Supplemental Fig. 5; Table 1). These data add support to the hypothesis that irreversible inhibition of EGFR and/or its ERBB family members may be important for achieving the most significant growth inhibition with PI3K and ERBB inhibitor combinations.

Discussion

Our data are consistent with previous studies showing the benefit of PI3K- and EGFR- inhibitor combination therapies (Rebucci et al., 2011; Young et al., 2013; D'Amato et al., 2014; Lattanzio et al., 2015; Michmerhuizen et al., 2016; Anisuzzaman et al., 2017; Silva-Oliveira et al., 2017) and also extend that work by discovering that PI3K inhibitors are much more effective in combination with irreversible than reversible EGFR inhibitors in HNSCC. In prior work comparing the classes of EGFR-targeting monotherapies in this cancer type, preclinical data demonstrated that irreversible EGFR inhibitors are superior to other EGFR-targeting agents, including cetuximab (Ather et al., 2013; Silva-Oliveira et al., 2017) and reversible inhibitor gefitinib (Young et al., 2015). Similarly, previous work has shown that the addition of ERBB2-targeting antibodies pertuzumab (Erjala et al., 2006) or trastuzumab (Kondo et al., 2008) to gefitinib enhances its efficacy in HNSCC cell lines; however, our findings demonstrated that the broader specificity of irreversible inhibitors alone cannot explain these differences in sensitivity, as administering ERBB2-inhibitor CP-724714 with gefitinib and HS-173 did not enhance drug effects (Fig. 3). Collectively, our data may suggest why greater improvements in patient survival after PI3K and EGFR combination therapies have not yet been observed in HNSCC and other cancers clinically and support the need for additional detailed studies of PI3K and EGFR combination therapies using irreversible ERBB inhibitors.

Of the published HNSCC studies evaluating PI3K and EGFR ditherapies, most have been performed with either cetuximab

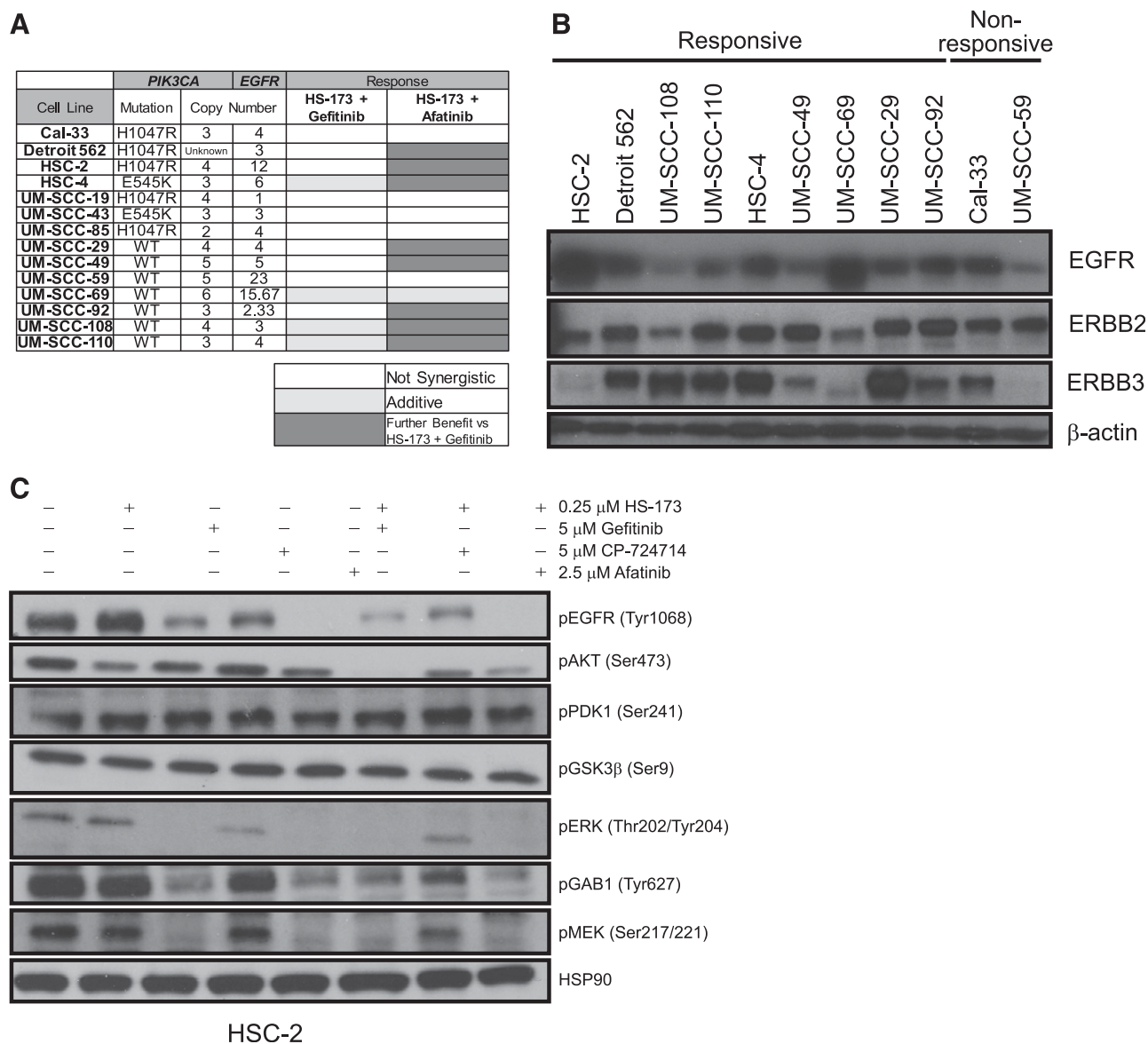


Fig. 5. Sensitivity of HNSCC cell lines to HS-173 and gefitinib or afatinib combination treatment. (A) Table shows mutation and copy-number data for cell lines tested for sensitivity to HS-173 and gefitinib or afatinib. *PIK3CA* mutations were confirmed via Sanger sequencing. No cell lines displayed mutations in *EGFR*. *PIK3CA* and *EGFR* copy number were determined using the publicly available canSAR database (Halling-Brown et al., 2012; Bulusu et al., 2014) for Cal-33, HSC-2, and HSC-4 cells and using OncoPrint for UM-SCC cells. Detroit 562 *EGFR* copy number was reported as previously published (Young et al., 2013). Combinatorial effects of HS-173 and gefitinib or afatinib were determined using resazurin cell viability assays after 72-hour drug treatment. Experiments with quadruplicate replicates were performed two to five times, and combination benefits were assessed using Combenefit software (Di Veroli et al., 2016) as described already. Four of 14 (29%) cell lines displayed additive effects after HS-173 and gefitinib cotreatment; eight of 14 (57%) models responded more favorably to combination treatment with HS-173 and afatinib. (B) Protein isolated from each cell line in the panel was used to perform Western blot analysis for EGFR, ERBB2, and ERBB3. β-actin was used as a loading control. (C) Western blot analysis of downstream PI3K and RAS-MEK-ERK pathway activation after 2-hour treatment with vehicle (DMSO), PI3Kα inhibitor HS-173, reversible EGFR inhibitor gefitinib, reversible ERBB2 inhibitor CP-724714, EGFR/ERBB2 inhibitor afatinib, or combinations in HSC-2 cells. HSP90 was used as a loading control. Representative images are shown.

(Rebucci et al., 2011; D'Amato et al., 2014; Lattanzio et al., 2015) or the reversible EGFR inhibitors (e.g., gefitinib, erlotinib) (Young et al., 2013; Anisuzzaman et al., 2017). One exception is a recent report from Silva-Oliveira et al. (2017) that examined the responses to PI3K pathway inhibitors (including AKT inhibitor MK-2206) with two different irreversible EGFR inhibitors. In this study, pharmacologic inhibition or siRNA knockdown of AKT resulted in improved sensitivity to afatinib and allitinib (a second irreversible EGFR inhibitor) in HN13 cells (Silva-Oliveira et al., 2017). The need to suppress

AKT phosphorylation in responses to PI3K + EGFR drug combinations is supported by studies of both EGFR-targeting antibodies (Benavente et al., 2009; Rebucci et al., 2011) and reversible inhibitors (Benavente et al., 2009; Rebucci et al., 2011; Young et al., 2013; Silva-Oliveira et al., 2017). In lung-cancer models, irreversible EGFR inhibitors have sustained reductions in EGFR phosphorylation and an improved ability to decrease effector AKT phosphorylation compared with reversible inhibitors (Kwak et al., 2005). The inability of reversible EGFR inhibitors to sustain suppression of EGFR

TABLE 1

Combinatorial effects of phosphatidylinositol 3-kinase (PI3K) + ERBB inhibitors in head and neck squamous cell carcinoma (HNSCC) cell lines

Combinatorial effects of PI3K α inhibitor HS-173 and reversible or irreversible ERBB-targeting agents in HSC-2 and Detroit 562 HNSCC cell lines. Synergy was assessed using Combobenefit software (Di Veroli et al., 2016). Synergy was not observed for PI3K α inhibitor HS-173 with any reversible inhibitor in either cell line. Four of four and three of four irreversible EGFR inhibitors were synergistic with HS-173 in HSC-2 and Detroit 562 cells, respectively.

Inhibitor	Target	Reversible/ Irreversible	HSC-2 Synergy	Detroit 562 Synergy
Gefitinib	EGFR	Reversible	No	No
Erlotinib	EGFR	Reversible	No	No
BMS-599626	EGFR/ERBB2	Reversible	No	No
CP-724714	ERBB2	Reversible	No	No
Afatinib	EGFR/ERBB2	Irreversible	Yes	Yes
TAK-285	EGFR/ERBB2	Irreversible	Yes	No
CUDC-101	EGFR/ERBB2/HDAC	Irreversible	Yes	Yes
Dacomitinib	EGFR/ERBB2/ERBB4	Irreversible	Yes	Yes

and AKT phosphorylation has been linked to altered receptor trafficking (Wiley, 2003), a mechanism that does not affect the activity of irreversible inhibitors. In contrast, we did not observe greater reductions in AKT phosphorylation with HS-173 and afatinib than with gefitinib dual therapy (Fig. 5C). These data suggest that factors other than or in addition to the level of suppression of downstream EGFR-effector signaling may be responsible for mediating combination benefit and/or that specific inhibitor combinations may be required to achieve synergistic cell-death responses.

Of the emerging novel classes of PI3K and EGFR inhibitors that we evaluated here, several are already in advanced clinical development for HNSCC and other cancers as monotherapy and combination therapies. For example, BKM120 improved survival when administered with paclitaxel (vs. paclitaxel and placebo) in a phase 2 HNSCC trial (Soulières et al., 2017), and BYL719 monotherapy demonstrated safety in patients with solid tumors (Juric et al., 2018). Of the irreversible EGFR inhibitors that we evaluated, dacomitinib has shown efficacy beyond that of cetuximab in preclinical models (Ather et al., 2013) and is undergoing evaluation in phase 2 studies in recurrent and metastatic HNSCC patients (NCT00768664, NCT01449201). Afatinib, although still indicated only for use in lung cancer patients, has also demonstrated similar efficacy to cetuximab (Seiwert et al., 2014) in HNSCC patients; this result is quite promising given that cetuximab was approved for use in HNSCC with radiation or cytotoxic chemotherapy after successful phase 3 trials (Bonner et al., 2006; Vermorken et al., 2008). Afatinib is currently undergoing evaluation in a variety of treatment paradigms in HNSCC (including NCT01824823, NCT01427478, NCT02979977, and NCT01783587) and has also been tested in other solid tumor types as part of a combination therapy with inhibitors targeting PLK (NCT01206816), Src (NCT01999985), insulin-like growth factor receptor (NCT02191891), MEK (NCT02450656), or multiple receptor tyrosine kinases (NCT00998296) but not yet with PI3K inhibitors.

Many irreversible EGFR inhibitors have activity against both wild-type and mutated forms of EGFR (including those with T790M and/or C797S resistance mutations), which may contribute to their improved clinical efficacy over reversible drugs like gefitinib and erlotinib. Thus, the use of irreversible EGFR inhibitors with PI3K inhibitors in HNSCC may lead

to more durable responses than reversible EGFR inhibitor combinations by eliminating not only EGFR mutations but also activation of compensatory signaling through PI3K as critical resistance mechanisms. Nevertheless, these combinations are still limited by other forms of resistance, including novel resistance mutations and co-dependent pathways, which will likely develop after prolonged exposure to even irreversible EGFR and PI3K inhibitor cotreatments.

Collectively, our work motivates the translation of specific PI3K and irreversible EGFR dual therapies into xenograft mouse models and other more clinically relevant systems. If such studies confirm our in vitro findings, clinical trials that evaluate these drug combinations will be warranted. More broadly, our data also motivate a need to develop additional biomarkers that can be used to determine not only whether a drug inhibits its target but also whether the drug inhibits pivotal downstream effector pathways capable of rescuing cell survival. Indeed, our findings suggest that responses may be mediated by complex downstream signaling networks or other yet-unidentified factors. Developing the next generation of adaptive biomarkers and rationally designed matched combination therapies may therefore be one key to improved survival for HNSCC patients.

Authorship Contributions

Participated in research design: Michmerhuizen, Carey, Brenner

Conducted experiments: Michmerhuizen, Leonard, Matovina, Harris, Herbst

Performed data analysis: Michmerhuizen, Kulkarni, Zhai, Jiang

Wrote or contributed to the writing of the manuscript: Michmerhuizen, Brenner

References

- Anisuzzaman AS, Haque A, Wang D, Rahman MA, Zhang C, Chen Z, Chen ZG, Shin DM, and Amin AR (2017) In vitro and in vivo synergistic antitumor activity of the combination of BKM120 and erlotinib in head and neck cancer: mechanism of apoptosis and resistance. *Mol Cancer Ther* 16:729–738.
- Ather F, Hamidi H, Fejzo MS, Letrent S, Finn RS, Kabbinnar F, Head C, and Wong SG (2013) Dacomitinib, an irreversible Pan-ERBB inhibitor significantly abrogates growth in head and neck cancer models that exhibit low response to cetuximab. *PLoS One* 8:e56112.
- Benavente S, Huang S, Armstrong EA, Chi A, Hsu KT, Wheeler DL, and Harari PM (2009) Establishment and characterization of a model of acquired resistance to epidermal growth factor receptor targeting agents in human cancer cells. *Clin Cancer Res* 15:1585–1592.
- Berenbaum MC (1981) Criteria for analyzing interactions between biologically active agents. *Adv Cancer Res* 35:269–335.
- Birkeland AC, Foltin SK, Michmerhuizen NL, Hoesli RC, Rosko AJ, Byrd S, Yanik M, Nor JE, Bradford CR, Prince ME, et al. (2017) Correlation of Crtc1/3-Maml2 fusion status, grade and survival in mucoepidermoid carcinoma. *Oral Oncol* 68:5–8.
- Birkeland AC, Yanik M, Tillman BN, Scott MV, Foltin SK, Mann JE, Michmerhuizen NL, Ludwig ML, Sandelski MM, Komarck CM, et al. (2016) Identification of targetable ERBB2 aberrations in head and neck squamous cell carcinoma. *JAMA Otolaryngol Head Neck Surg* 142:559–567.
- Bliss CI (1939) The toxicity of poisons applied jointly. *Ann Appl Biol* 26:585–615.
- Boeckx C, Baay M, Wouters A, Specenier P, Vermorken JB, Peeters M, and Lardon F (2013) Anti-epidermal growth factor receptor therapy in head and neck squamous cell carcinoma: focus on potential molecular mechanisms of drug resistance. *Oncologist* 18:850–864.
- Bonner JA, Harari PM, Giralt J, Azarnia N, Shin DM, Cohen RB, Jones CU, Sur R, Raben D, Jassem J, et al. (2006) Radiotherapy plus cetuximab for squamous-cell carcinoma of the head and neck. *N Engl J Med* 354:567–578.
- Borisy AA, Elliott PJ, Hurst NW, Lee MS, Lehar J, Price ER, Serbedzija G, Zimmermann GR, Foley MA, Stockwell BR, et al. (2003) Systematic discovery of multicomponent therapeutics. *Proc Natl Acad Sci USA* 100:7977–7982.
- Brenner JC, Graham MP, Kumar B, Saunders LM, Kupfer R, Lyons RH, Bradford CR, and Carey TE (2010) Genotyping of 73 UM-SCC head and neck squamous cell carcinoma cell lines. *Head Neck* 32:417–426.
- Bulusu KC, Tym JE, Coker EA, Schierz AC, and Al-Lazikani B (2014) canSAR: updated cancer research and drug discovery knowledgebase. *Nucleic Acids Res* 42:D1040–D1047.
- D'Amato V, Rosa R, D'Amato C, Formisano L, Marciano R, Nappi L, Raimondo L, Di Mauro C, Servetto A, Fuscillo C, et al. (2014) The dual PI3K/mTOR inhibitor PKI-587 enhances sensitivity to cetuximab in EGFR-resistant human head and neck cancer models. *Br J Cancer* 110:2887–2895.

- Di Veroli GY, Fornari C, Wang D, Mollard S, Bramhall JL, Richards FM, and Jodrell DI (2016) Combeneft: an interactive platform for the analysis and visualization of drug combinations. *Bioinformatics* **32**:2866–2868.
- Erjala K, Sundvall M, Junttila TT, Zhang N, Savisalo M, Mali P, Kulmala J, Pulkkinen J, Grenman R, and Elenius K (2006) Signaling via ERBB2 and ERBB3 associates with resistance and epidermal growth factor receptor (EGFR) amplification with sensitivity to EGFR inhibitor gefitinib in head and neck squamous cell carcinoma cells. *Clin Cancer Res* **12**:4103–4111.
- Giefing M, Wierzbicka M, Szyfter K, Brenner JC, Braakhuis BJ, Brakenhoff RH, Bradford CR, Sorensen JA, Rinaldo A, Rodrigo JP, et al. (2016) Moving towards personalised therapy in head and neck squamous cell carcinoma through analysis of next generation sequencing data. *Eur J Cancer Res* **12**:147–157.
- Gillison ML, Chaturvedi AK, Anderson WF, and Fakhry C (2015) Epidemiology of human papillomavirus-positive head and neck squamous cell carcinoma. *J Clin Oncol* **33**:3235–3242.
- Greco WR, Bravo G, and Parsons JC (1995) The search for synergy: a critical review from a response surface perspective. *Pharmacol Rev* **47**:331–385.
- Halling-Brown MD, Bulusu KC, Patel M, Tym JE, and Al-Lazikani B (2012) canSAR: an integrated cancer public translational research and drug discovery resource. *Nucleic Acids Res* **40**:D947–D956.
- Jimeno A, Shirai K, Choi M, Laskin J, Kochenderfer M, Spira A, Cline-Burkhardt V, Winquist E, Hausman D, Walker L, et al. (2015) A randomized, phase II trial of cetuximab with or without PX-866, an irreversible oral phosphatidylinositol 3-kinase inhibitor, in patients with relapsed or metastatic head and neck squamous cell cancer. *Ann Oncol* **26**:556–561.
- Juric D, Rodon J, Tabernero J, Janku F, Burris HA, Schellens JHM, Middleton MR, Berlin J, Schuler M, Gil-Martin M, et al. (2018) Phosphatidylinositol 3-kinase α -selective inhibition with alpelisib (BYL719) in PIK3CA-altered solid tumors: results from the first-in-human study [published correction appears in *J Clin Oncol* (2019) 37:361]. *J Clin Oncol* **36**:1291–1299.
- Kamangar F, Dores GM, and Anderson WF (2006) Patterns of cancer incidence, mortality, and prevalence across five continents: defining priorities to reduce cancer disparities in different geographic regions of the world. *J Clin Oncol* **24**:2137–2150.
- Kondo N, Ishiguro Y, Kimura M, Sano D, Fujita K, Sakakibara A, Taguchi T, Toth G, Matsuda H, and Tsukuda M (2008) Antitumor effect of gefitinib on head and neck squamous cell carcinoma enhanced by trastuzumab. *Oncol Rep* **20**:373–378.
- Kwak EL, Sordella R, Bell DW, Godin-Heymann N, Okimoto RA, Brannigan BW, Harris PL, Driscoll DR, Fidias P, Lynch TJ, et al. (2005) Irreversible inhibitors of the EGF receptor may circumvent acquired resistance to gefitinib. *Proc Natl Acad Sci USA* **102**:7665–7670.
- Lattanzio L, Tonissi F, Monteverde M, Vivenza D, Russi E, Milano G, Merlano M, and Lo Nigro C (2015) Treatment effect of buparlisib, cetuximab and irradiation in wild-type or PI3KCA-mutated head and neck cancer cell lines. *Invest New Drugs* **33**:310–320.
- Lee H, Jung KH, Jeong Y, Hong S, and Hong SS (2013) HS-173, a novel phosphatidylinositol 3-kinase (PI3K) inhibitor, has anti-tumor activity through promoting apoptosis and inhibiting angiogenesis. *Cancer Lett* **328**:152–159.
- Li D, Ambrogio L, Shimamura T, Kubo S, Takahashi M, Chirieac LR, Padera RF, Shapiro GI, Baum A, Himmelsbach F, et al. (2008) BIBW2992, an irreversible EGFR/HER2 inhibitor highly effective in preclinical lung cancer models. *Oncogene* **27**:4702–4711.
- Liu J, Pan S, Hsieh MH, Ng N, Sun F, Wang T, Kasibhatla S, Schuller AG, Li AG, Cheng D, et al. (2013) Targeting Wnt-driven cancer through the inhibition of porcupine by LGK974. *Proc Natl Acad Sci USA* **110**:20224–20229.
- Ludwig ML, Birkeland AC, Hoelsli R, Swiecicki P, Spector ME, and Brenner JC (2016) Changing the paradigm: the potential for targeted therapy in laryngeal squamous cell carcinoma. *Cancer Biol Med* **13**:87–100.
- Ludwig ML, Kulkarni A, Birkeland AC, Michmerhuizen NL, Foltin SK, Mann JE, Hoelsli RC, Devenport SN, Jewell BM, Shuman AG, et al. (2018) The genomic landscape of UM-SCC oral cavity squamous cell carcinoma cell lines. *Oral Oncol* **87**:144–151.
- Lui VW, Hedberg ML, Li H, Vangara BS, Pendleton K, Zeng Y, Lu Y, Zhang Q, Du Y, Gilbert BR, et al. (2013) Frequent mutation of the PI3K pathway in head and neck cancer defines predictive biomarkers. *Cancer Discov* **3**:761–769.
- Lynch TJ, Bell DW, Sordella R, Gurubhagavatula S, Okimoto RA, Brannigan BW, Harris PL, Haserlat SM, Supko JG, Haluska FG, et al. (2004) Activating mutations in the epidermal growth factor receptor underlying responsiveness of non-small-cell lung cancer to gefitinib. *N Engl J Med* **350**:2129–2139.
- Mathews Griner LA, Guha R, Shinn P, Young RM, Keller JM, Liu D, Goldlust IS, Yasgar A, McKnight C, Boxer MB, et al. (2014) High-throughput combinatorial screening identifies drugs that cooperate with ibrutinib to kill activated B-cell-like diffuse large B-cell lymphoma cells. *Proc Natl Acad Sci USA* **111**:2349–2354.
- Michmerhuizen NL, Leonard E, Kulkarni A, and Brenner JC (2016) Differential compensation mechanisms define resistance to PI3K inhibitors in PIK3CA amplified HNSCC. *Otorhinolaryngol Head Neck Surg* **1**:44–50.
- Murugan AK, Munirajan AK, and Tsuchida N (2013) Genetic deregulation of the PIK3CA oncogene in oral cancer. *Cancer Lett* **338**:193–203.
- Ozanne B, Richards CS, Hendler F, Burns D, and Gusterson B (1986) Over-expression of the EGF receptor is a hallmark of squamous cell carcinomas. *J Pathol* **149**:9–14.
- Paez JG, Jänne PA, Lee JC, Tracy S, Greulich H, Gabriel S, Herman P, Kaye FJ, Lindeman N, Boggon TJ, et al. (2004) EGFR mutations in lung cancer: correlation with clinical response to gefitinib therapy. *Science* **304**:1497–1500.
- Rebucci M, Peixoto P, Dewitte A, Wattez N, De Nuncques MA, Rezvoy N, Vautravere-Dewas C, Buisine MP, Guerin E, Peyrat JP, et al. (2011) Mechanisms underlying resistance to cetuximab in the HNSCC cell line: role of AKT inhibition in bypassing this resistance. *Int J Oncol* **38**:189–200.
- Rodon J, Braña I, Siu LL, De Jonge MJ, Homji N, Mills D, Di Tomaso E, Sarr C, Trandafir L, Massacesi C, et al. (2014) Phase I dose-escalation and -expansion study of buparlisib (BKM120), an oral pan-class I PI3K inhibitor, in patients with advanced solid tumors. *Invest New Drugs* **32**:670–681.
- Rumman M, Jung KH, Fang Z, Yan HH, Son MK, Kim SJ, Kim J, Park JH, Lim JH, Hong S, et al. (2016) HS-173, a novel PI3K inhibitor suppresses EMT and metastasis in pancreatic cancer. *Oncotarget* **7**:78029–78047.
- Seiwert TY, Fayette J, Cupissol D, Del Campo JM, Clement PM, Hitt R, Degardin M, Zhang W, Blackman A, Ehrnrooth E, et al. (2014) A randomized, phase II study of afatinib versus cetuximab in metastatic or recurrent squamous cell carcinoma of the head and neck. *Ann Oncol* **25**:1813–1820.
- Shum D, Radu C, Kim E, Cajuste M, Shao Y, Seshan VE, and Djaballah H (2008) A high density assay format for the detection of novel cytotoxic agents in large chemical libraries. *J Enzyme Inhib Med Chem* **23**:931–945.
- Silva-Oliveira RJ, Melendez M, Martinho O, Zanon MF, de Souza Viana L, Carvalho AL, and Reis RM (2017) AKT can modulate the *in vitro* response of HNSCC cells to irreversible EGFR inhibitors. *Oncotarget* **8**:53288–53301.
- Soulières D, Faivre S, Mesia R, Remenar É, Li SH, Karpenko A, Dechaphunkul A, Ochsenreither S, Kiss LA, Lin JC, et al. (2017) Buparlisib and paclitaxel in patients with platinum-pretreated recurrent or metastatic squamous cell carcinoma of the head and neck (BERIL-1): a randomised, double-blind, placebo-controlled phase 2 trial. *Lancet Oncol* **18**:323–335.
- Thress KS, Paweletz CP, Felip E, Cho BC, Stetson D, Dougherty B, Lai Z, Markovets A, Vivancos A, Kuang Y, et al. (2015) Acquired EGFR C797S mutation mediates resistance to AZD9291 in non-small cell lung cancer harboring EGFR T790M. *Nat Med* **21**:560–562.
- Tillman BN, Yanik M, Birkeland AC, Liu CJ, Hovelson DH, Cani AK, Palanisamy N, Carskadon S, Carey TE, Bradford CR, et al. (2016) Fibroblast growth factor family aberrations as a putative driver of head and neck squamous cell carcinoma in an epidemiologically low-risk patient as defined by targeted sequencing. *Head Neck* **38** (Suppl 1):E1646–E1652.
- Vermorken JB, Mesia R, Rivera F, Remenar E, Kawecki A, Rottey S, Erfan J, Zabolotnyy D, Kienzer HR, Cupissol D, et al. (2008) Platinum-based chemotherapy plus cetuximab in head and neck cancer. *N Engl J Med* **359**:1116–1127.
- Wiley HS (2003) Trafficking of the ErbB receptors and its influence on signaling. *Exp Cell Res* **284**:78–88.
- Wu SG, Liu YN, Tsai MF, Chang YL, Yu CJ, Yang PC, Yang JC, Wen YF, and Shih JY (2016) The mechanism of acquired resistance to irreversible EGFR tyrosine kinase inhibitor-afatinib in lung adenocarcinoma patients. *Oncotarget* **7**:12404–12413.
- Young NR, Liu J, Pierce C, Wei TF, Grushko T, Olopade OI, Liu W, Shen C, Seiwert TY, and Cohen EE (2013) Molecular phenotype predicts sensitivity of squamous cell carcinoma of the head and neck to epidermal growth factor receptor inhibition. *Mol Oncol* **7**:359–368.
- Young NR, Soneru C, Liu J, Grushko TA, Hardeman A, Olopade OI, Baum A, Solca F, and Cohen EE (2015) Afatinib efficacy against squamous cell carcinoma of the head and neck cell lines *in vitro* and *in vivo*. *Target Oncol* **10**:501–508.
- Yu HA, Arcila ME, Rekhtman N, Sima CS, Zakowski MF, Pao W, Kris MG, Miller VA, Ladanyi M, and Riely GJ (2013) Analysis of tumor specimens at the time of acquired resistance to EGFR-TKI therapy in 155 patients with EGFR-mutant lung cancers. *Clin Cancer Res* **19**:2240–2247.
- Yu HA, Tian SK, Drlon AE, Borsu L, Riely GJ, Arcila ME, and Ladanyi M (2015) Acquired resistance of EGFR-mutant lung cancer to a T790M-specific EGFR inhibitor: emergence of a third mutation (C797S) in the EGFR tyrosine kinase domain. *JAMA Oncol* **1**:982–984.

Address correspondence to: Dr. J. Chad Brenner, Department of Otolaryngology-Head & Neck Surgery, University of Michigan, 1150 E. Medical Center Drive, 9301B MSRB3, Ann Arbor, MI 48109-0602. E-mail: chadbren@umich.edu

**Rationale for using irreversible EGFR Inhibitors in combination with PI3K inhibitors for
advanced Head and Neck Squamous Cell Carcinoma**

Nicole L. Michmerhuizen, Elizabeth Leonard, Chloe Matovina, Micah Harris,

Gabrielle Herbst, Aditi Kulkarni, Jingyi Zhai, Hui Jiang, Thomas E. Carey, J. Chad Brenner

Molecular Pharmacology

Table S1. Primary Antibody Conditions

Target	Supplier	Cat. No.	Dilution
pEGFR(Tyr1068)	Cell Signaling Technology	3777	1:1000
EGFR	Origene	TA312545	1:2000
pERBB2(Tyr1221/1222)	Cell Signaling Technology	2249	1:500
ERBB2	Cell Signaling Technology	2165	1:1000
pMEK(Ser217/221)	Cell Signaling Technology	9121	1:1000
MEK1/2	Cell Signaling Technology	8727	1:1000
pERK1/2(Thr202/Tyr204)	Cell Signaling Technology	4370	1:1000
ERK1/2	Cell Signaling Technology	4695	1:1000
pAKT(Ser473)	Cell Signaling Technology	4060	1:1000
AKT	Cell Signaling Technology	4685	1:1000
HSP90	Cell Signaling Technology	4877	1:2000
β -actin	Cell Signaling Technology	4970	1:2000

Figure S1. Sanger sequencing confirmed E545K *PIK3CA* mutation in UM-SCC-43 and HSC-4 cells and H1047R *PIK3CA* mutation in Cal-33, HSC-2, Detroit 562, UM-SCC-19 and UM-SCC-85 cells.

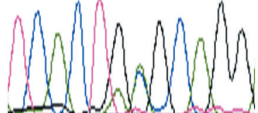

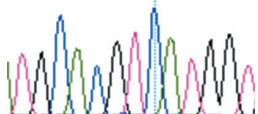
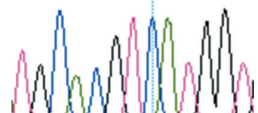
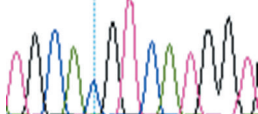
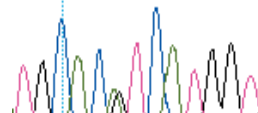
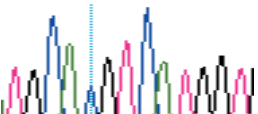
Figure S2. HSC-2 cells were treated with increasing concentrations of pan-PI3K inhibitor BKM120 (A), PI3K α inhibitor BYL719 (B), or PI3K β inhibitor TGX-221 (C) and/or EGFR/ERBB2 inhibitor afatinib for 72 hours. Cell viability was measured using a resazurin cell viability assay. Each point is the mean and s.d. of quadruplicate determinations from a single experiment. Each experiment was repeated independently at least two times with similar combination effects; representative data is shown along with analysis using Combenefit software (Di Veroli et al., 2016).

Figure S3. Detroit 562 (A, C) and HSC-4 (B, D) cells were treated with increasing concentrations of EGFR/ERBB2 inhibitor afatinib and/or pan-PI3K inhibitor BKM120 (A, B) or PI3K α inhibitor HS-173 (C, D) for 72 hours. Cell viability was measured using a resazurin cell viability assay. Each point is the mean and s.d. of quadruplicate determinations from a single experiment. Each experiment was repeated independently two times with similar combination effects; representative data is shown along with analysis using Combenefit software (Di Veroli et al., 2016).

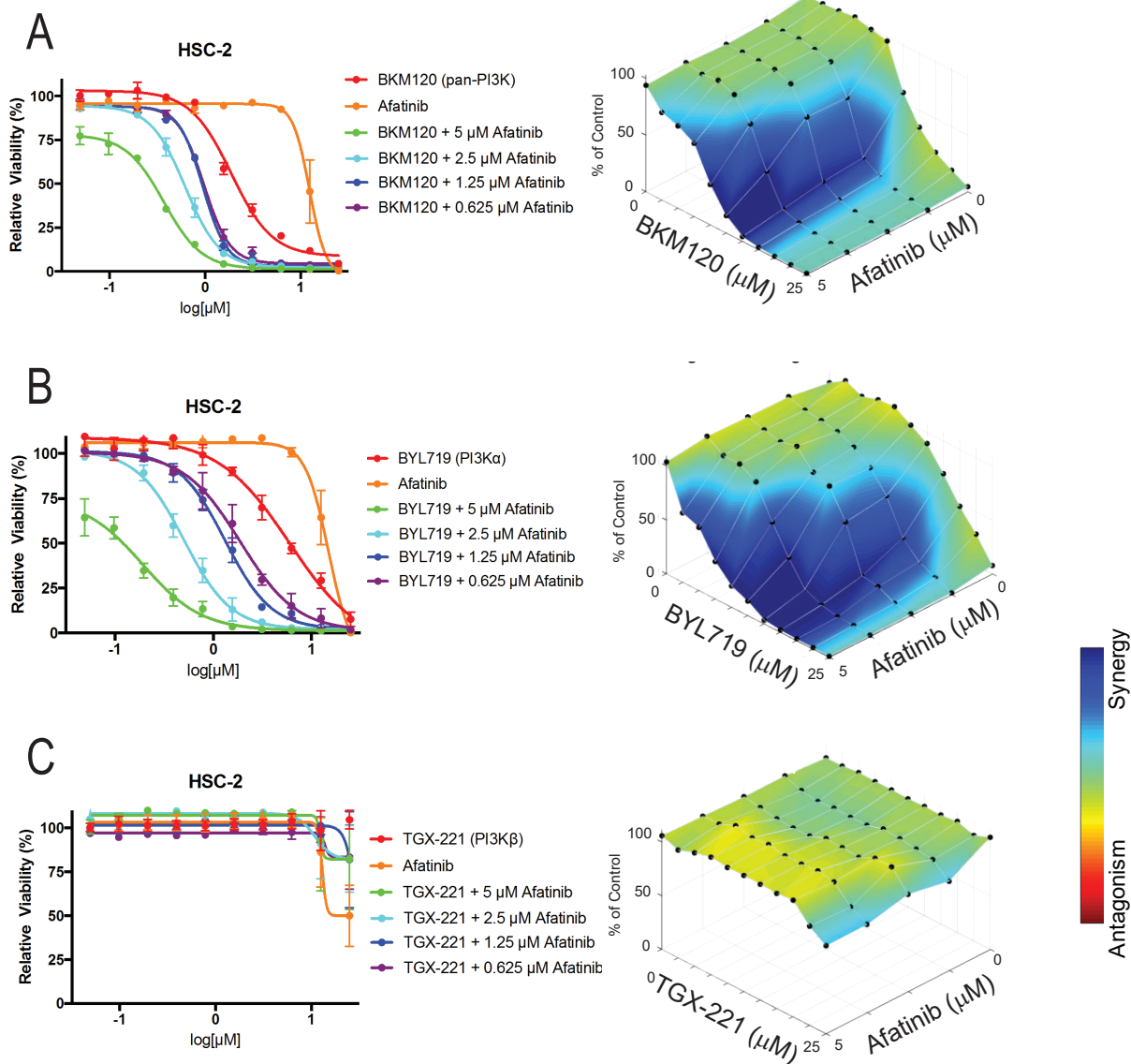
Figure S4. UM-SCC-110 and matched fibroblasts from the same patient (UM-SCC-110 fibroblasts) were treated with vehicle (DMSO), PI3K α inhibitor HS-173 and/or EGFR/ERBB2 inhibitor afatinib for 72 hours. Cell viability was measured using a resazurin cell viability assay. Data shown is the mean and s.d. of duplicate determinations.

Figure S5. HSC-2 cells were treated with increasing concentrations of PI3K α inhibitor HS-173 and/or reversible EGFR inhibitor erlotinib (A), reversible EGFR/ERBB2 inhibitor BMS-599626, irreversible EGFR/ERBB2 inhibitor TAK285, or irreversible EGFR/ERBB2 inhibitor CUDC-101 (D) for 72 hours. Cell viability was measured using a resazurin cell viability assay. Each point is the mean and s.d. of quadruplicate determinations from a single experiment. Each experiment was repeated independently at

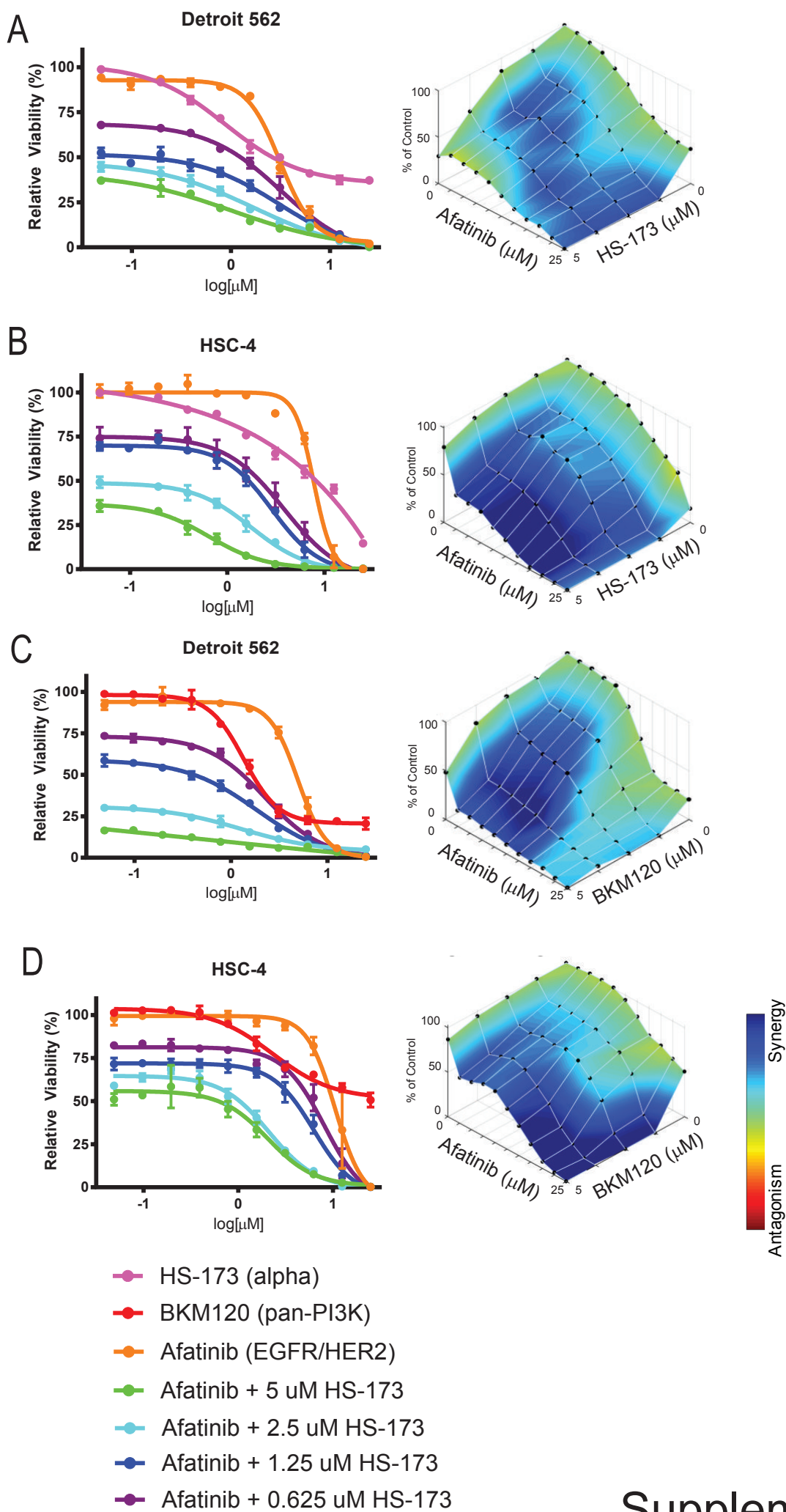
least two times with similar combination effects; representative data is shown along with analysis using Combenefit software (Di Veroli et al., 2016).

	Primer (5'-3')		Chromatogram
UM-SCC-43 c.1633G>A E545K	F	CATCTGTGAATCCAGAGGGGA	<u>TCACTGAGCAGG</u> Reference 
	R	AACATGCTGAGATCAGCCAAA	TCACT <u>A</u> AGCAGG Cell Line
HSC-4 c.1633G>A E545K	F	CATCTGTGAATCCAGAGGGGA	<u>TCACTGAGCAGG</u> Reference 
	R	AACATGCTGAGATCAGCCAAA	TCACT <u>A</u> AGCAGG Cell Line
Cal-33 c.3014A>G H1047R	F	GCTCCAAACTGACCAAAGTGT	<u>TGCACATCATGGT</u> Reference 
	R	AATCGGTCTTTGCCTGCTGA	TGCAC <u>G</u> TCATGGT Cell Line
HSC-2 c.3014A>G H1047R	F	GCTCCAAACTGACCAAAGTGT	<u>TGCACATCATGGT</u> Reference 
	R	AATCGGTCTTTGCCTGCTGA	TGCAC <u>G</u> TCATGGT Cell Line
Detroit 562 c.3014A>G H1047R	F	GCTCCAAACTGACCAAAGTGT	<u>TGCACATCATGGT</u> Reference 
	R	AATCGGTCTTTGCCTGCTGA	TGCAC <u>G</u> TCATGGT Cell Line
UM-SCC-85 c.3014A>G H1047R	F	GCTCCAAACTGACCAAAGTGT	<u>TGCACATCATGGT</u> Reference 
	R	AATCGGTCTTTGCCTGCTGA	TGCAC <u>G</u> TCATGGT Cell Line
UM-SCC-19 c.3014A>G H1047R	F	GCTCCAAACTGACCAAAGTGT	<u>TGCACATCATGGT</u> Reference 
	R	AATCGGTCTTTGCCTGCTGA	TGCAC <u>G</u> TCATGGT Cell Line

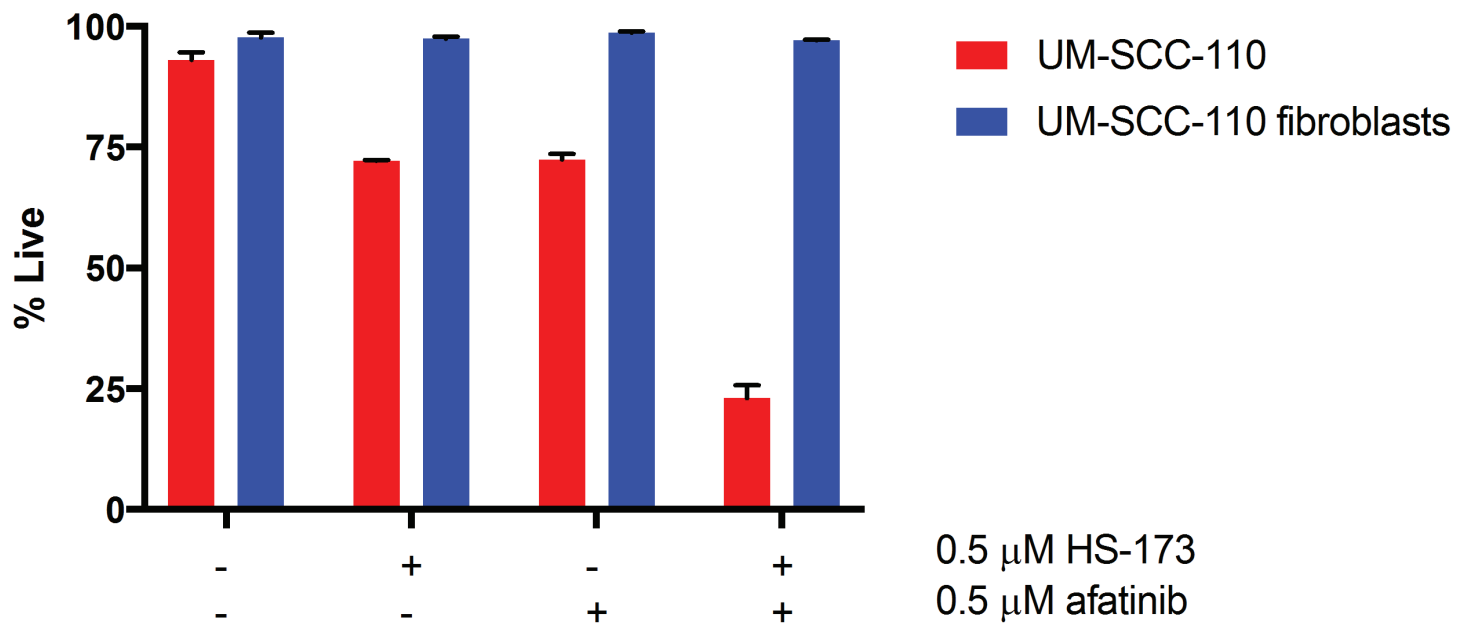
Supplementary Figure 1



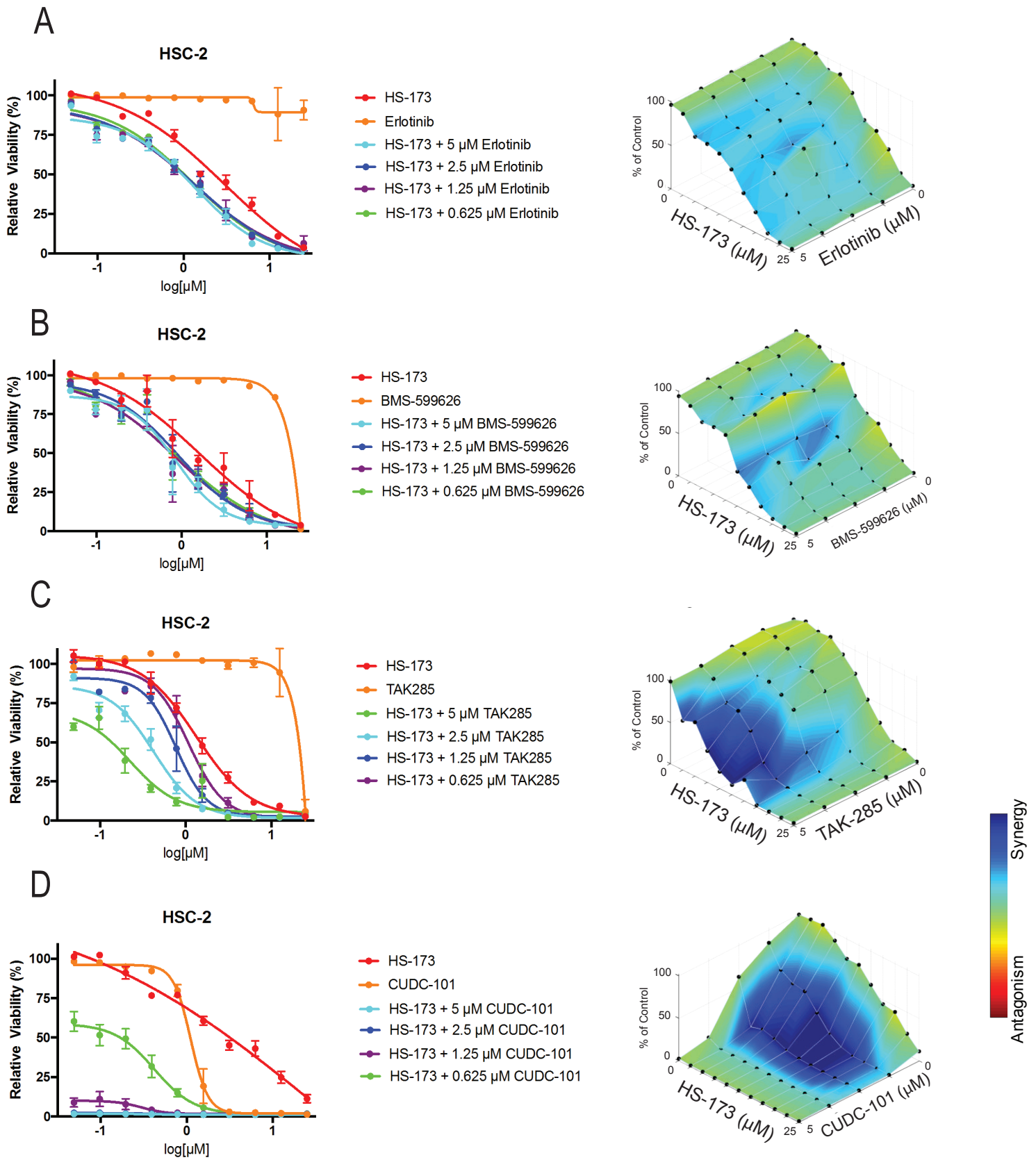
Supplementary Figure 2



Supplementary Figure 3



Supplementary Figure 4



Supplementary Figure 5